Friction drag measurements in turbulent wall flows

AIMETA 2017
XXIII Conference
The Italian Association of Theoretical and Applied Mechanics
Luigi Ascione, Valentino Berardi, Luciano Feo, Fernando Fraternali and Antonio Michele Tralli (eds.)
Salerno, Italy, 4-7 September 2017

FRICTION DRAG MEASUREMENTS IN TURBULENT WALL FLOWS

G. Iuso[1], S. Sedda[1], M. Pesando[1], C. Sardu[1]

[1] Politecnico di Torino – Mechanical and Aerospace Department
Corso Duca degli Abruzzi 24, 10129 Torino
gaetano.iuso@polito.it

Keywords: riblets, friction drag measurement, wall turbulence, flow control.

Keywords: friction drag measurement, wall turbulence, riblets.

Abstract. *Results of an experimental investigation devoted to the assessment of methodologies aimed at the friction drag measurement in turbulent wall flows are presented. Two techniques for local measurements have been developed. Namely, different versions of the velocity profile method have been used for a turbulent boundary layer developing on a flat plate. The oil flow interferometer has been arranged and results related with measurements performed in a fully developed turbulent channel flow and in the turbulent boundary layer are presented. Moreover a balance based on a floating-buoyancy system finalized to the integral measurement of the friction force acting on the flat plate is presented. The results of the three techniques are compared considering as a reference a well assessed empirical law. Good level of measurement accuracy using the balance has been evidenced highlighting the capability of the balance for the characterization of micro-grooved surfaces addressed for friction drag reduction applications.*

1 INTRODUCTION

The riblets technology aimed at the friction drag reduction continues to maintain high the interest of the scientific community due to the beneficial effects especially in case of application in the aeronautical field. The riblets technique is a passive solution appeared in the early 80' year [1],[2]. Recent works [3],[4] confirm the beneficial effects and open new perspectives. The great problem that remain to solve for a large scale application of the riblet techniques is the manufacturing of the reliable grooves on large surfaces [5],[6].

From an experimental point of view the friction drag characterization due to the presence of micro-roughness requires an accurate technique for the evaluation of the such drag. These evaluations can be performed locally using probes or with analytical methods or it can be carried out globally by means of direct measurements using a balance. An exhaustive overview on the measurement techniques devoted for the skin friction is reported by Winter [7]. Fernholz et al. [8], Naughton and Sheplak [9] focused on local measurements describing MEMS-based sensors, oil film interferometry and liquid crystal coatings.

Wall similarity techniques are widely used for the local evaluation of the wall shear stress making use of the velocity distribution in turbulent boundary layer. One of the first methods which exploits the local mean velocity profile and the log-law is due to Clauser [10]. Baron and Quadrio [11] proposed a modified slope method based on the wall similarity capable of accurate evaluation of friction velocity on smooth and grooved surfaces.

The drag balances directly measure the integrated force due to the wall stress distribution on the surface of the floating element. Acharya et al. [12] employed a reduced size floating element instrumented upon a precision galvanometer to measure friction drag in a turbulent boundary layer. Specifically designed and manufactured by Bechert et al. [13] is an oil channel for the drag reduction investigations on large flat plate. An original balance with large floating element, 3 meter long by 1 meter width, was used by Krishna et al.[14]. The authors measured the displacement of the sensor element that was translated into a force measurement by a load cell. More detailed analysis was performed by Baars et al. [15] that accurately validated the balance reported in [14]. A sufficiently large floating plate is particularly indicated in the case of investigation on surfaces with roughness because it allows the development of equilibrium condition of the wall flow. Another direct measurement of the wall friction for a local evaluation is the oil film interferometry. This technique is reliable and very attractive because is free from calibration and without any assumption about the flow. In fact the technique can be applied to flow characterized by pressure gradient, wall curvature, 3D boundary layers among others. The determination of the local shear stress is based on the observation of an oil film stretched out by the wall flow that exhibit a system of interference fringes. Squire [16] developed the mathematical treatment of the evolution of a thin oil film. First applications are due to Tanner and Blows [17], Monson [18]. Investigation on airfoils using oil film interferometer technique was performed by Driver [19] and Driver and Drake [20]. Application in a fully developed channel flow was also performed by Zurlo et al. [21]. Some drawbacks also characterize this technique such as the oil contamination and the presence of dust on the surface. Moreover the determination of the fringe spacing requires particular attention due to the intrinsic uncertainty present in measurements. Chauhan et al. [22] in their work analyzed a mode decomposition and the Hilbert transform for a more accurate evaluation of the fringe spacing.

In this paper different measurements techniques are presented devoted for local and integral skin friction evaluation developing in wall turbulent flows. Oil film interferometry is assessed in a fully developed turbulent channel flow and also applied for the case of a turbulent boundary layer developing on a flat plate. Wall similarity methods were as well considered for the boundary layer experiment. Moreover a floating balance for direct measurement of the friction force

acting on a large floating plate is presented. Comparison of the results pertaining to the different investigations is performed.

2 EXPERIMENTAL SET UP

In the following, the channel flow and the wind tunnel are described along with the measurements techniques devoted for the skin friction force evaluation.

2.1 Wind tunnel and channel flow facilities

The wind tunnel is of blowing type with large diffuser mounted just downstream of two fans positioned at the inlet. A large settling chamber links the exit of the rapid diffuser with the entry of the convergent characterized by a 12:1 contraction ratio. The test section is 4 meters long while the cross area has width and height equal to 0.7m and 0.5m respectively. In figure 1a the picture of the wind tunnel is shown. At the exit of the test section a corner with a turning vane deviates vertically upward the flow. In this region an adjustable plate allows the control of the longitudinal pressure gradient in the test section to reach a nominal zero pressure gradient condition. The velocity in the test section can be varied up to 30 m/sec.

a) b)

Figure 1. Wind tunnel and plane channel

The plane channel has a length equal to 8 meters and the cross section has height and width equal to 30mm and 420mm respectively, which determine a width to eight ratio equal to 14 that ensures a 2D flow in a considerable extension in the spanwise direction. Furthermore, the overall length is sufficient to ensure a fully developed flow in the test section. A centrifugal blower provide to set the flow rate according to the desired flow condition to be tested. The cross section of the channel is linked to the exit of the blower through a settling chamber and a convergent. The Reynolds number based on the friction velocity ranges from 50 to 2000. Along the centerline of the channel 45 pressure taps are distributed for the pressure distribution measurement. A pressure transducer DAS3217 form Scanivalve provide the simultaneous readings of 16 selected pressure taps signals for the pressure distribution measurements. Each of the 16 inputs has a thermo-compensated piezo resistive transducer characterized by FS=±2400Pa and accuracy equal to =±0.05%FS. The maximum sampling speed is equal to 500Hz/channel. A LAN connection links the pressure transducer directly to a pc. The test section where measurements are performed is positioned downstream the entrance at a distance equal to 6 meter from the inlet. The upper wall of the cross section is larger than the channel width allowing the transversal movement in order to investigate the flow in the spanwise direction when probes are used. In figure 1b the picture of the channel is displayed.

2.2 Oil film interferometry: channel flow application and data reduction

A first experiment was arranged in the plane channel setting different fully developed flows. In this apparatus the oil flow interferometer (OFI) technique was used. The end of this investigation was to assess accurately the experimental set up of the oil flow interferometer technique, the tuning of measurements parameters and the post processing of the data for a reliable evaluation of the skin friction. From this point of view the channel flow is a robust reference flow for the accurate assessment of the interferometer technique. In fact it was possible to verify the level of accuracy comparing the skin friction evaluated using the oil film method with those of the channel flow based on the pressure gradient measurement. For a fully developed channel flow wall shear stress and pressure gradient are linked by the relation:

$$\tau_w = \left|\frac{\mathrm{d}p}{\mathrm{d}x}\right| \frac{H}{2}$$

Once the optical technique was well assessed it was employed in the boundary layer investigation for the comparison with the other techniques, namely the wall similarity law and the balance for direct measurement.

The equipment used in the present experiment for the oil film interferometer techniques, widely employed in laboratories, consists in a simple arrangement composed by a lamp, a camera and appropriate oil. The illuminating system require a monochromatic light and we chose a sodium vapor lamp with a wavelength λ=589nm. The oil has to be characterized by some peculiarities recommended in bibliography. Silicon oil are suggested due to the very low sensitivity of the viscosity to the temperature and also due to the large index of refraction. Oils with different viscosity are available and the specific choice is related with the strength of the wall shear stress.

In the experiments, we used oil from Dow Corning highly used for this measurements. In particular we employed oil with viscosity equal to 10cSt for low Reynolds number and 50 and 100cSt for increasing Reynolds numbers. The cameras usually used are of CCD type. We adopted a Nikon D3300 with a resolution of 24Mpixels coupled with an optic having a focal length equal to 105mm. Camera frame-rate, focalization and light sensitivity are managed with the open source program digiCamControl®. A last requirement is linked with the optical properties of the wall under investigation that must be as smooth as possible to avoid disturbances on the developing film. Even the presence of small particles of dust on the surface influence locally the shape of the fringes. In the case of sufficiently thin oil film a linear relationship holds between the thinning rate and the shear force acting upon it. The thickness of the oil film is most easily measured using the interferometer technique that allow the generation of fringes in the oil film. Following the evolution of the oil drop in the stage of thin film over the surface it is possible to correlate the thinning rate and the shear stress according to the relation given by Marusic et al. [23]

$$\tau_w = 2m\frac{\mu}{\lambda}\sqrt{n_o^2 - n_{air}^2 sin\vartheta_i^2} \qquad 1$$

where m is the growing rate of the fringe spacing while μ is the oil viscosity, λ is the light wavelength, n_o and n_{air} represent the oil and the air refraction index respectively. Finally θ_i is the incidence angle of the light. The only quantity to be measured to determine the wall shear stress is m being all the remaining parameters known. The quantity m expresses the time variation of the fringes spacing defined as:

$$m = \frac{(\Delta x_{t_{n+1}} - \Delta x_{t_n})}{(t_{n+1} - t_n)}$$

In this relation $\Delta x_{t_{n+1}}$ and Δx_{t_n} represent the fringes spacing evaluated from two consecutive images recorded at the time instants t_{n+1} and t_n respectively. The instantaneous spacing was first evaluated developing a MATLAB® code based on a sinusoidal interpolation used by White [24]. In figure 2 an example of the fringe pattern is shown. The flow is from top to down.

Figure 2. Example of instantaneous fringes pattern generated in the oil film and selected area.

As can be seen, crossing the fringes the variation of the light intensity have a periodic behaviour tending towards a sinusoidal form with a period that corresponds to the fringes spacing. In figure 3a an example of the light intensity distribution along the x coordinate having origin at the head of the oil film is displayed for a sample captured at the time instant t_0.

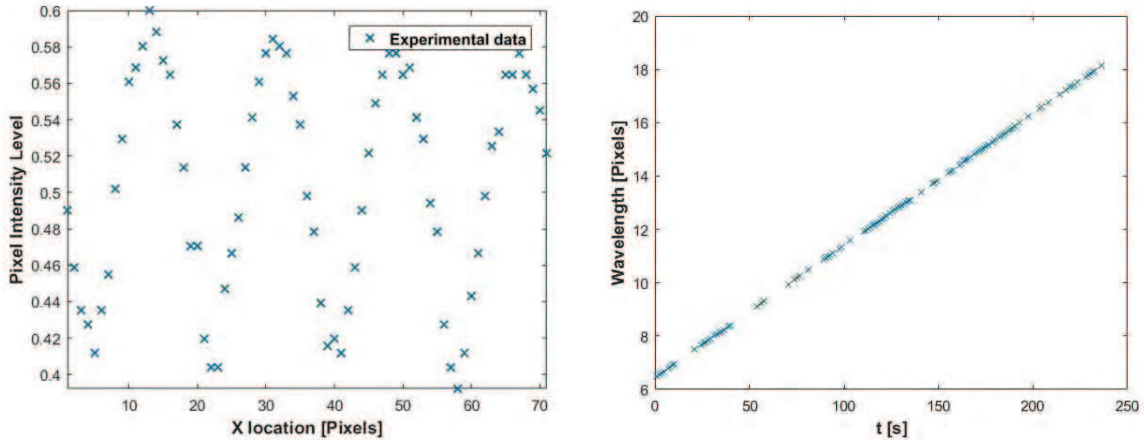

a) b)

Figure 3. a) Periodic light variations crossing the fringes at the time t_0 b) Time evolution of the fringes spacing deriving from the analysis of all the images.

A Matlab® script fits a four-parameter sine wave of the form $f(x)=C_1\sin(C_2 x+C_3)+C_4$ to the data set by using a function which minimizes the rms error between the values of the data set and the sine wave. The constant C_1 represents the amplitude of the sine wave, C_3 is a phase shift, C_4 is an offset from the x axis and represents an average pixel intensity value. C_2 represents the space frequency, or wavelength (in pixels) of the sine wave. This is the most important parameter because it corresponds to the fringe spacing. In figure 3b the wavelength of the spacing (i.e. the fringe spacing) as a function of the time evaluated from the complete set of images is shown. As can be seen the time behaviour of the fringe spacing is linear and the slope *m* is easily evaluated.

2.3 Flat plate turbulent boundary layer: experimental set up and wall similarity methods

The second experiment was set up in the wind tunnel for the investigation of the turbulent boundary layer over a flat plate. the measurements of the boundary layer velocity profiles are

performed Only on a part of the flate plate . This part is also made independent from the larger and fixed plate that cover the whole width of the test section and can float in the flow direction. Upstream, in proximity of the convergent the fixed plate is linked with the lower wall of the test section using a double curvature shape that reduces the test section cross section to an effective height of 0.3 meters. In figure 4 detail of the test section and of the floating plate is displayed. This last component is the core "sensor" of the skin friction balance that will be described in detail in the next section.

Mean velocity distributions in the turbulent boundary layer were measured in various streamwise positions at the centerline of the floating plate using a flattened total pressure probe with external thickness equal to 0.85mm. A positioning system motorized with a stepper motor remotely controlled provided the displacement of the probe along the boundary layer. The static pressure was measured through the pressure taps realized on the fixed part of the plate, adjacent to the floating element. A capacitive pressure transducer 239E model by SETRA, with a full scale equal to ±0.2PSID and accuracy equal to ±0.14%FS provided the measurements of the dynamic pressure for the velocity evaluation. In addition to the pressure taps in the streamwise direction, two lines of pressure taps were disposed also in the transverse directions to check the pressure gradient. The readings of the pressure were carried out using a Scanivalve ZOC33 combined with the SmartZOC directly connected via LAN with a computer. The Zoc33 allows the simultaneous measurement of up to 64 pressure channels, with a full scale equal to ±10inch H_2O and an accuracy equal to ±0.08%FS. The reading of the SETRA pressure transducer signal was sampled using a NI data acquisition system composed by a cDAQ-9172 main frame and a NI9239 module having an A/D resolution equal to 24 bit.

The near wall measurements using a total pressure probe suffer from the effects introduced by the velocity shear across the inlet of the tube and from the blockage of the probe. To this end the measured data of the total probe were corrected using the procedure indicated by Bailey et al. [25]. In the following figure 4c the total pressure probe is displayed along with the floating flat plate.

A large variety of techniques based on the wall similarity are present in the literature. The majority of these methods are based on the logarithmic velocity distribution in the inner part of the turbulent boundary layer developing in condition of zero pressure gradient and fully developed flow. Namely, in that region the law describing the velocity distribution is given in the non-dimensional form as follows:

$$\frac{u}{u_\tau} = \frac{1}{k}\ln\left(\frac{y u_\tau}{\nu}\right) + C$$

where k and C are the von Karman and Coles constants. We assumed for such constants values equal to 0.41 and 5 respectively according to the literature data. The term u_τ is the friction velocity and y is wall normal distance.

We followed two procedures for the skin friction evaluation. The first procedure is based on the modified slope method centered on the log law as reported by Baron and Quadrio [11]. Moreover we consider the van Driest relation [26] that express the non-dimensional velocity distribution valid from the viscous sublayer up to the end of the logarithmic region.

The main problem underlying the use of the logarithmic law is the reliable identification of the log region in the experimental data plotted in semi logarithmic plane. Baron and Quadrio identified the central point of the log region considering that it is coincident with the inflection point of the velocity distribution. Nevertheless, a sufficient number of experimental data are necessary to be identified around the central point for the accurate evaluation of the constant slope region of the velocity distribution to which the friction velocity is strictly related. Instead

of evaluating the slope for a continuous increasing number of N points around the inflection point, as done by Baron and Quadrio[11], we defined a different number of points on the left and right side of the inflection point that are inside the constant slope range. All the experimental data in the semi-logaritmic plane were first fitted using a 8th order polynomial. The definition of of this analytical function allowed the identification of the inflection point.. The authors prefer this procedure because the location of the inflection point is influenced from the Reynolds number. In fact this point moves towards the buffer layer as the Reynolds number increases. In addition the extensions of the logarithmic region increases. For these reasons, at high Raynolds numbers it is preferable to consider more points towards the outer layer direction. This influence was tested using the data base of Osterlund [27]. Furthermore, the eventual presence of an overshoot of the velocity distribution makes more difficult the identification of the log region in its lower part. The overshoot velocity behavior is well documented in the literature and Monkewitz [28] gave an analytical expression for the bump of the velocity. For each combination of the left and right points a Matlab® routine provides the value of the unknown friction velocity through an optimization procedure given the values of the constants k and C. Some analysis were also performed considering as unknowns both the friction velocity and the offset of the initial value of the distance from the wall Δy_o in the log law. As a reference for the estimation the classic Clauser method was also considered for a preliminary estimation of the local friction coefficient.

The second procedure relies on the van Driest equation, which has the advantage of a unique formulation valid from the viscous sublayer up to the end of the logarithmic region. The van Driest velocity distribution is expressed as:

$$u^+ = \int_0^{y^+} \frac{2y^+}{b + \sqrt{b^2 + 4a(y^+)}} \quad \text{where} \quad \left\{ \begin{array}{c} a(y^+) = \left[ky^+ \left(1 - \exp\left(-\frac{y^+}{c^+} \right) \right) \right]^2 \\ b = 1 \\ c^+ = 26 \end{array} \right\}$$

In this case it is necessary to identify only the upper limit of the log region. To this end we educed form the experimental data a second inflection point that is positioned in the region between the upper part of the log region and the initial part of the outer layer. Starting from this point we eliminate an increasing number of experimental data, towards the logarithmic region, and for each of the remaining points the Matlab® program provide the estimation of the friction velocity through the same previous optimization method. The inflection points, whichever is the methods, are clearly visible if the velocity data points are plotted in a semi-log plane u(y)-y.

2.4 Balance for integrated skin friction measurement

The idea underling the design of a balance for the direct measurement of the integral friction force derives from the solution adopted by Krishna et al. [14] that used a large floating plate (3meter x 1meter), which suspension was guaranteed by a system of four air bearings applying a pressure equal to 80psi. In the present design we exploited a hydraulic system for the buoyancy and the floating of the inner plate. Four water reservoirs mounted on the wall of the wind tunnel generate the buoyancy needed by the floating apparatus that supports the plate under investigation. The level of the water in the reservoirs is adjustable, adding or removing water, in order to ensure the alignment between the fixed and the floating plate. On both sides of the floating apparatus two LVDT sensors are symmetrically mounted for the measurement of the displacement of the test plate under the action of the friction force acting on its surface. The

displacement are translated in the friction force through calibration curves. The displacement sensors have high accuracy equal to 0.5% FS corresponding to ±12.5μm, that means ±0.7 viscous length at a free stream velocity equal to 20m/sec.. Between the floating plate and the empty cylinder a labyrinth system made of small channels was inserted to minimize the leakage effects through the unavoidable gaps present around the floating plate. In figure 4 some pictures of the components of balance are shown.

a) b) c)

Figure 4. a) Water reservoirs and empty cylinders b) LVDT sensors and floating system c) Floating plate.

The vertical position of the floating plate was measured by mean of a laser displacement sensor mounted on the wind tunnel wall just in the center of the lower part of the plate.

For an accurate evaluation of the friction drag the spurious effects of the longitudinal pressure gradient have to be taken also into account. In fact the presence of a longitudinal pressure gradient introduces a buoyancy force directed as the free stream velocity that directly affects the drag. The resulting pressure gradient longitudinal force is related to the volume of the floating body and to the pressure gradient as follow:

$$F_p = \left|\frac{dp}{dx}\right| \cdot V$$

Nominally on the flat plate the pressure gradient is equal to zero, but due to the configuration of the experiment a residual slight pressure gradient can be present, although attention and precaution are considered in the realization. Therefore this pressure gradient has to be measured and considered in the evaluation of the friction force. To this end the pressure taps along the fixed part of the plate have provided the measurement of the pressure gradient for each test.

3 RESULTS

In the following the results related with both experiments using the different techniques are presented. Moreover a comparative analysis of the results is shown.

In figure 5 results of the wall shear stress measured by means of the OFI technique and using the values of the pressure gradient in the channel flow are reported. These results are showed in terms of non dimensional pressure drop versus the Reynolds number of the channel based on the centerline velocity and the hydraulic diameter of the channel. In the same diagram also the analytical laws for the laminar and the turbulent regimes are displayed as reference.

The level of accordance between the results of the two techniques is considerable. Also a good agreement between the experimental data with respect to the friction laws from the literature is attested. In the transitional regime the measurement are less accurate due to the not regular evolution of the drop under the flow intermittency behavior in this regime.

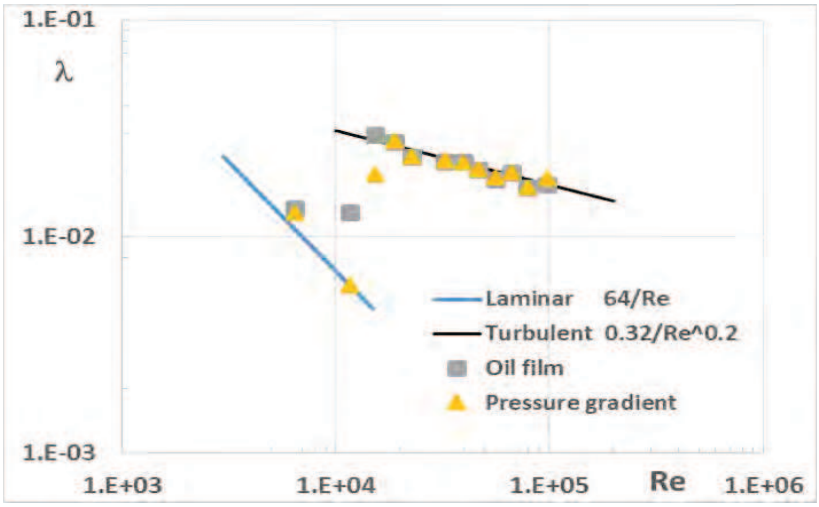

Figure 5. Channel flow: oil film and pressure gradient skin friction comparison.

For the oil film interferometer technique the uncertainty analysis on the evaluation of the skin friction oil film was performed according the study of Moffat [29]. The relation for this investigation follows the error propagation and is given below:

$$\delta\tau_w = \sqrt{\sum_{j=1}^{N}\left(\frac{\partial\tau_w}{\partial k_j}\delta k_j\right)^2}$$

The contributions due to the refraction indexes and to the wavelength of the light were fixed to zero because we assumed them without uncertainty and in any case the influence tested is very small. Only the contributions related with the dependence of the skin friction from the viscosity, from the growth rate of the fringes spacing m and from the incidence angle of the light θ were considered. In figure 6 the amount of the three contribution under the square root for five Reynolds numbers ranging from 10^4 to $1.3{\cdot}10^5$ are displayed. The uncertainties δk_j for temperature, the angle of incidence of the light were defined according to the instrumentations used. For these two last parameters the uncertainty were respectively $\delta T = 0.1°$ and $\delta\vartheta = 0.2°$ and were fixed for all the tests. The uncertainty δm linked to the growth rate of the fringe spacing, was evaluated considering the linear regression of the experimental data and the rule for the estimation of the slope uncertainty. This last uncertainty is Reynolds dependent and has been taken into account in the final uncertainties results reported in the following figure 6.

As can be observed the most critical contribution is the ones linked with the effect of the viscosity due to its dependence from the temperature. In fact it is evident that the viscosity-temperature effect has for all the Reynolds numbers the greatest value, at least one order of magnitude higher than the others contributions. A sensitivity analysis was also performed regarding the temperature effect. To obtain an error less than 1% in the measurement of the skin friction the uncertainties on the temperature measurement should be of the order of 0.01°.

This result gives also a warning on the fact that also the ambient temperature during the tests should be monitored accurately.

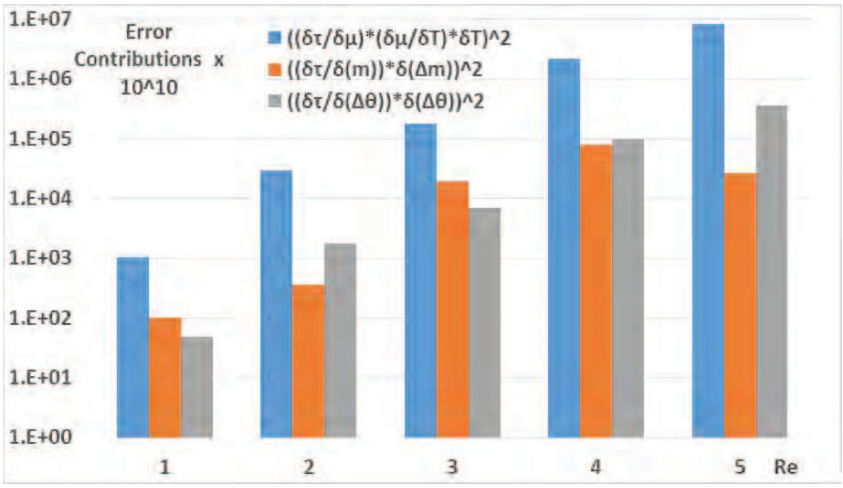

Figure 6. Channel flow: oil film and pressure gradient skin friction comparison.

By summing the contributions of the all the uncertainties the percentage error on the skin friction measurements was evaluated. These results are reported in figure 7. As can be seen the uncertainty is of the order of 2% for low Reynolds number and then it reduces as the Reynolds number increases.

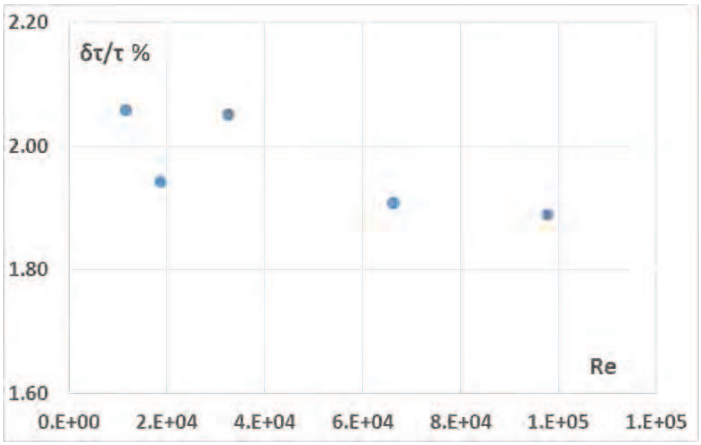

Figure 7. Percentage error on the skin friction measurements for different Reynolds numbers.

Some examples of results concerning the wall similarity methods are reported below for the velocity distribution measured in the central point of the floating plate. The virtual origin of this plate without a true leading edge was estimated comparing the drag coefficient measured by the balance and that evaluated using a well-assessed empirical relation from the literature:

$$C_f = 0.0576/(Re_x)^{0.2}$$

In figure 8 in the semi logarithmic plane is displayed the velocity distribution of all the experimental data points as continuous line. The inflectional point shown in red and positioned in the log region also the In particular in figure 8a we consider two points of the left side (NL=2) and three point on the right side (NR=3) of the inflectional point while in figure 8b we accounted for NL=3 and NR=4.

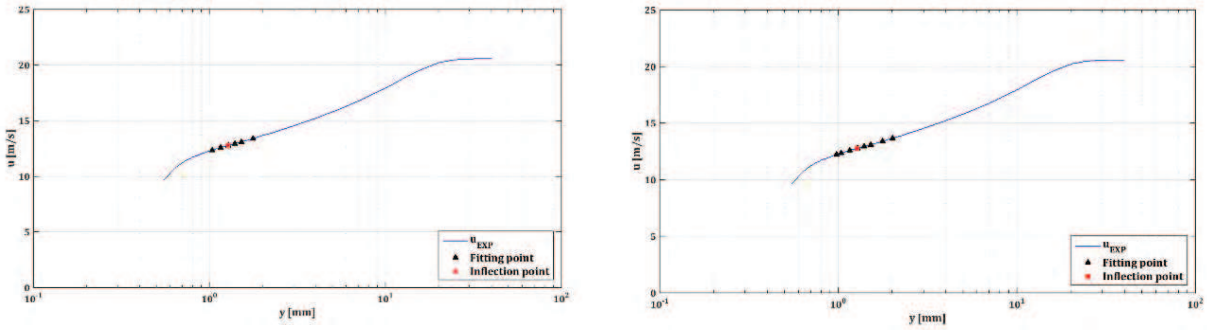

a) b)

Figure 8. Dimensional velocity distributions and chosen data points. a) N_L=2 – N_R=3 b) N_L=3 – N_R=4.

On the base of the data points identified for the two case a Matlab routine provided the respective values of the friction velocity used for the plot $u^+=f(y^+)$ shown in figure 9. In the same figure 9 the laws corresponding to the dashed lines represent the linear behavior in the viscous sublayer and the log law other than the van Driest law.

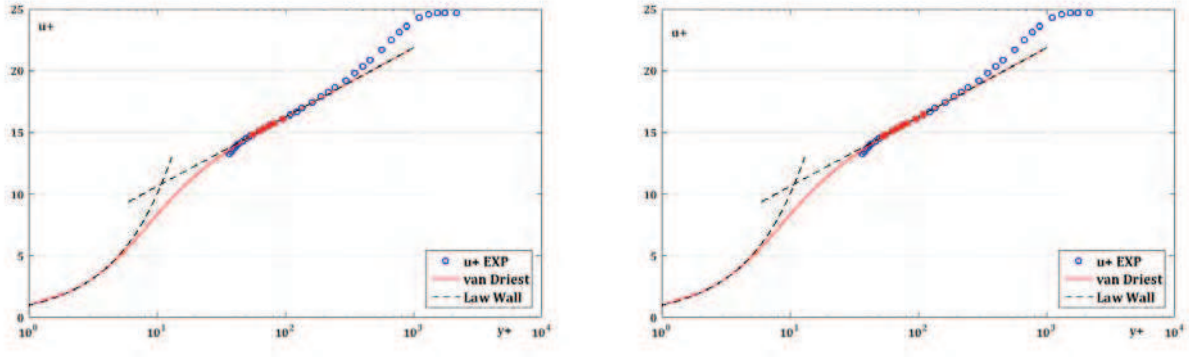

a) b)

Figure 9. Velocity distributions using the wall law. Chosen data points: a) N_L=2 – N_R=3 b) N_L=3 – N_R=4.

As can be seen from figure 9b, the data points, N_L and N_R, around the inflectional point identify exactly the log region that subsequently exploited allows the evaluation of the friction velocity. For both cases the friction velocity is almost identical as will be reported in the final table below. In figure 10 the results relatively to the van Driest method are shown. The upper inflectional point is visible in figure 10a while in the semi-log plane $u^+=f(y^+)$ is displayed the experimental data and the laws described before.

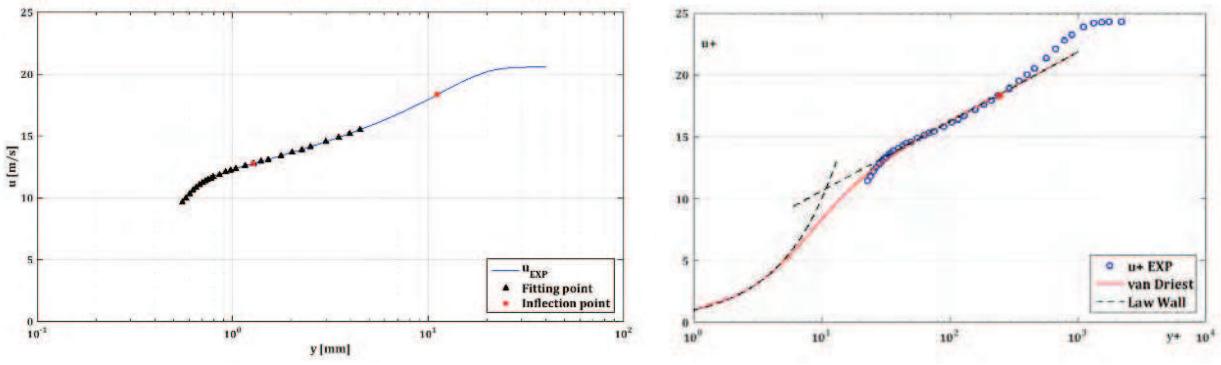

a) b)

Figure 10. Velocity distributions using van Driest equation. Data points eliminated on the left side -5.

Also for this method, the remaining data point allows to evaluate the friction velocity with a certain degree of accuracy fitting the van Driest relation. Some discrepancies arise between the experimental data and the van Driest relation in the velocity overshoot region where the analytical relation do not taken into account the presence of this bump of velocity. In table 1 the values of the friction velocity has been reported for the methods tested.

Method	Data points Left	Data points Right	u_τ [m/s]	%Err_u_τ
Log law with inflection point	2	3	8.329E-01	1.230E+00
	2	4	8.329E-01	1.227E+00
	3	3	8.330E-01	1.233E+00
	3	4	8.329E-01	1.229E+00
van Driest	-4	0	8.467E-01	2.902E+00
	-5	0	8.463E-01	2.853E+00
Clauser			8.310E-01	9.935E-01
Empirical Law 0.0576/Rex ^(1/5)			8.228E-01	0.000E+00

Table 1. Friction velocities and percentage errors.

In the same table as reference, we report also the results obtained using the empirical relation introduced before. As can be seen from the table the results from the log law method are almost the same whichever is the number of data points considered. The best results for this method appears for the combination N_L=2 and N_R=4. Instead, van Driest relation highlights friction velocity characterized by the highest error close 3%. The low accuracy of the van Driest method with respect to the others can be due to the presence of the bump in the experimental velocity distribution located in the near wall region that is not considered by the van Driest equation. The Clauser method is not surprising that gives the best results in absolute because of the visual optimization process that allows the fine tuning of the friction coefficient.

The measurements performed by the skin friction floating balance were compared with those of the oil film technique and those of the Clauser method. In figure 11 these results in terms of drag coefficient as a function of the Reynolds number are shown. Moreover the values deriving from the empirical relation are reported in the same figure as reference.

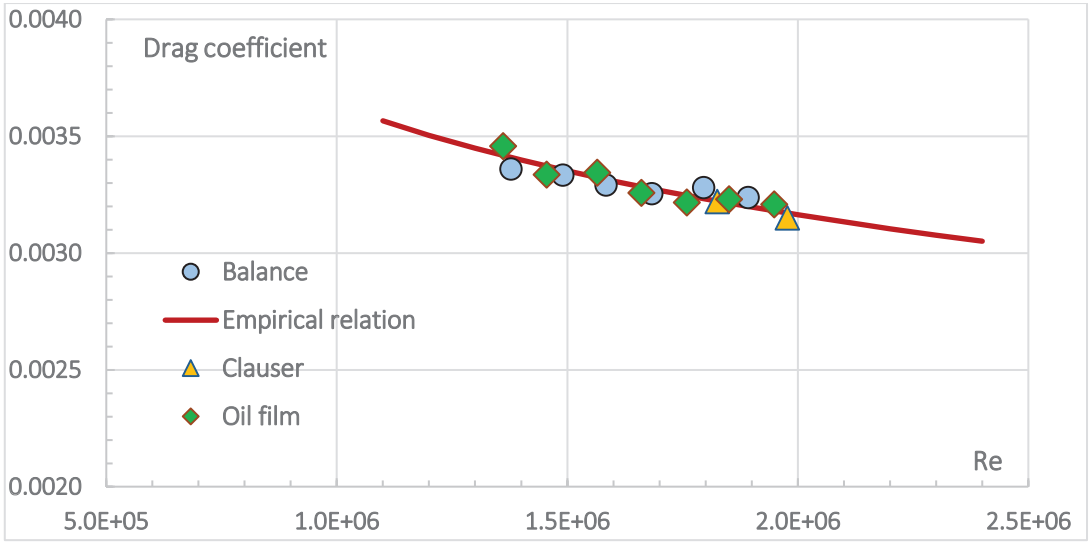

Figure 11. Comparison of the drag coefficients evaluated by different techniques.

As can be observed the results of the three experimental techniques are in good agreement between each other. Moreover all the results collapse on the curve of the empirical law. In particular the balance have showed a good level of assessment and reliability and this is important for the next investigation on plates having surface with riblets micro grooves.

4 CONCLUSIONS

Different wall shear stress measurements techniques have been investigated devoted for local and integrated evaluation. The objective of this work is to set up reliable methods to be applied in investigation focused on the friction drag reduction using grooved surfaces. Oil film interferometry technique and the modified wall similarity techniques have been considered for the local evaluation of the skin friction. Moreover also the van Driest relation and the classical Clauser method have been tested. The design and the performances of a balance based on a large floating plate have been presented. The optical technique has been validate in a channel flow experiment and then applied in the turbulent boundary layer experiment developing on a flat plate as reference technique being robust, accurate and free from calibration. For the boundary layer experiment on the floating plate the skin friction measurements techniques have been used and the results have been compared. A very good agreement of the results emerges for the comparison between the different techniques. In particular the balance shows a maximum deviation of the order of 2.5% respect to the empirical law.

ACKNOWLEDGEMENTS

The authors are grateful to the student Lutri for the collaboration and the work developed during his final project. Also appreciations are due to the technicians Marco Cannata and Marco Grivet for their help for solving hardware problems.

This research has received funding from the European Community's Seventh Framework Programme (FP7/2007-2013) for the Clean Sky Joint Technology Initiative (Grant agreement CSJU-GAM-GRA-2008-001) and the European Community's Horizon 2020 - the Framework Programme for Research and Innovation (2014-2020) for the Clean Sky Joint Technology Initiative (Grant agreement CS2-REG-GAM-2014-2015-01).

REFERENCES

[1] M. J. Walsh and L. M. Weinstein. Drag and heat-transfer characteristics of small longitudinally ribbed surfaces. *AIAA Journal*, 1979, 17:770–771.

[2] D.W. Bechert, M. Bruse, W. Hage, J.G.T. van der Hoeven, and G. Hoppe. Experiments on dragreducing surfaces and their optimization with an adjustable geometry. *Journal of Fluid Mechanics,* 1997, 338:59–87.

[3] P. R. Spalart and J. D. McLean. Drag reduction: enticing turbulence, and then an industry. *Philosophical Transactions of the Royal Society*, 2011, A, 369:1556–1569.

[4] R. Tognaccini,B. Mele, P. Catalano, D. De Rosa, G. Iuso, S. Sedda, M. Ventre. Riblets: Ready for application on next generation aircrafts? *Proceedings in Greener Aviation GA2016*, Bruxelles, October 2016

[5] H. Kordy. Process abilities of the riblet-coating process with dual-cure lacquers. *CIRP Journal of Manufacturing Science and Technology,*2015,11:1–9.

[6] W. Hage, V. Stenzel, and T. Vynnyk. Investigation of the wear properties of a riblet paint structure on an airbus A300-600ST Beluga, *New Results in Numerical and Experimental Fluid Mechanics VIII,* 2013,Vol. 121 pages 185–192. Springer,

[7] K. Winter, An outline of the techniques available for the measurement of skin friction in turbulent boundary layers. *Progress in Aerospace Sciences,* vol. 18, pp. 1-57, 1977.

[8] H. H.Fernholz, G., Janke, M.Schober, D. Wagner New developments and applications of skin-friction measuring techniques, *Meas. Sci. Technology, 7,* 1996,1396-1409

[9] J.W. Naughton, M. Sheplak, Modern developments in shear-stress measurements. *Progress in Aerospace Sciences* 2002, 38 515–570

[10] F.H. Clauser, Turbulent boundary layers in adverse pressure gradients. *Journal of the Aeronautical Sciences*, vol. 21, no. 2, pp. 91-108, 1954

[11] Baron, M. Quadrio, On the Accuracy of Wall Similarity Methods in Determining Friction Velocity Over Smooth and Ribletted Surfaces. *J. Fluid Engineering,* December 1997, vol.119, pp.1009-1011

[12] Acharya M., Bornstein J., Escudier M.P. and V. Vokurka, Development of a floating element for the measurement of a surface shear stress. *AIAA Journal*, March 1985, vol. 23, No. 3

[13] D.W. Bechert, Hoppe G., J.G.T. van der Hoewen, and R. Makris, The Berlin oil channel for drag reduction research. *Experiments in Fluids* 1992,12, 251-260,

[14] T. M. Krishna, C. M. de Silva, I. Marusic, New drag balance facility for skin-friction studies in turbulent boundary layer at high Reynolds numbers, *17th Australasian Fluid Mechanics Conference* Auckland, New Zealand, December 5-9, 2010

[15] W. J. Baars, D. T. Squire, K. M. Talluru, M. R. Abbassi , N. Hutchins, I. Marusic, Wall-drag measurements of smooth- and rough-wall turbulent boundary layers using a floating element, *Experiments in Fluids* (2016) 57:90

[16] L. Squire, The motion of a thin oil sheet under the steady boundary layer on a body, *Journal of Fluid Mechanics,* 11, 1961, 161-179.

[17] L. H. Tanner, L.G. Blows, A study of the motion of oil films on the surfaces in air flow with application to the measurements of skin friction, *Journal of Physics E: Scientific Instruments,* 9, 1976, 194-202.

[18] D.J. Monson, A non instrusive laser interferometer method for measurement of skin friction, *Experiments in Fluids* 1, 1983, 15-22.

[19] D.M. Driver, Application of oil-film interferometry skin-friction measurements to large wind tunnel, *Experiments in Fluids,* 2003, 717-725.

[20] D.M. Driver, A. Drake, Skin friction measurements using oil-film interferometry in NASA's 11-foot transonic wind tunnel, *AIAA October 2008 Vol.46, No.10*.

[21] N. Zurlo, G. Iuso, G.M. Di Cicca, M. Onorato, Misura di sforzo d'attrito a parete per mezzo di tecnica interferometrica. *XV Congresso Nazionale AIDDA* Vol. I, 1999

[22] K. Chauhan, H.C.H. Ng, I. Marusic, , Empirical mode decomposition and Hilbert transforms for analysis of oil-film interferograms, *Meas. Sci. Technology,* 21, 2010, 105405 (13pp)

[23] Marusic I., Monty J.P, Hutchins N., Chong M.S. Oil film interferometry in high Reynolds number turbulent boundary layers. *16th Australasian Fluid Mechanics Conference,* 2007.

[24] White J.C. High-frame-rate Oil film interferometry. *Thesis* presented to the Faculty of California Polytechnic State University, San Luis Obispo, 2011.

[25] S. C. C. Bailey, M. Hultmark, J. P. Monty, P. H. Alfredsson, M. S. Chong, R. D. Duncan, J. H. M. Fransson, N. Hutchins, I. Marusic, B. J. McKeon, H. M. Nagib, R. Örlü, A. Segalini, A. J. Smits, R. Vinuesa, Obtaining accurate mean velocity measurements in high Reynolds number turbulent boundary layers using Pitot tubes, *J. Fluid Mech. (2013),* vol. 715, pp. 642_670.

[26] V. Driest, On turbulent flow near a wall, *J. Aerospace Science*, 1956, 23, pp 1007-1011.

[27] J.M. Osterlund, Experimental studies of zero pressure-gradient turbulen boundary layer flow, *Doctoral thesis* , Stockholm 1999, Royal Institute of Technology–Department of Mechanics

[28] P.A. Monkewitz, K.A. Chauhan, H.M. Nagib Self-consistent high Reynolds number asymptotics for zero-pressure-gradient turbulent boundary layers, *Phys Fluids* 2007, 19(11):1–12

[29] R. J. Moffat, Contributions to the theory of single-sample uncertainty analysis. *ASME, Transactions, Journal of Fluids Engineering* 1982,104.2 : 250-258.